



Identification of the role of DAB2 and CXCL8 in uterine spiral artery remodeling in early-onset preeclampsia

Yu Liu¹ · Lili Du¹ · Shifeng Gu¹ · Jingying Liang¹ · Minshan Huang¹ · Lijun Huang¹ · Siying Lai¹ · Shuang Zhang¹ · Zhaowei Tu¹ · Wei Sun¹ · Dunjin Chen¹ · Jingsi Chen^{1,2} 

Received: 13 November 2023 / Revised: 27 January 2024 / Accepted: 18 March 2024
© The Author(s) 2024

Abstract

Aberrant remodeling of uterine spiral arteries (SPA) is strongly associated with the pathogenesis of early-onset preeclampsia (EOPE). However, the complexities of SPA transformation remain inadequately understood. We conducted a single-cell RNA sequencing analysis of whole placental tissues derived from patients with EOPE and their corresponding controls, identified DAB2 as a key gene of interest and explored the mechanism underlying the communication between Extravillous trophoblast cells (EVTs) and decidual vascular smooth muscle cells (dVSMC) through cell models and a placenta-decidua coculture (PDC) model in vitro. DAB2 enhanced the motility and viability of HTR-8/SVneo cells. After exposure to conditioned medium (CM) from HTR-8/SVneo^{shNC} cells, hVSMCs exhibited a rounded morphology, indicative of dedifferentiation, while CM-HTR-8/SVneo^{shDAB2} cells displayed a spindle-like morphology. Furthermore, the PDC model demonstrated that CM-HTR-8/SVneo^{shDAB2} was less conducive to vascular remodeling. Further in-depth mechanistic investigations revealed that C-X-C motif chemokine ligand 8 (CXCL8, also known as IL8) is a pivotal regulator governing the dedifferentiation of dVSMC. DAB2 expression in EVT is critical for orchestrating the phenotypic transition and motility of dVSMC. These processes may be intricately linked to the CXCL8/PI3K/AKT pathway, underscoring its central role in intricate SPA remodeling.

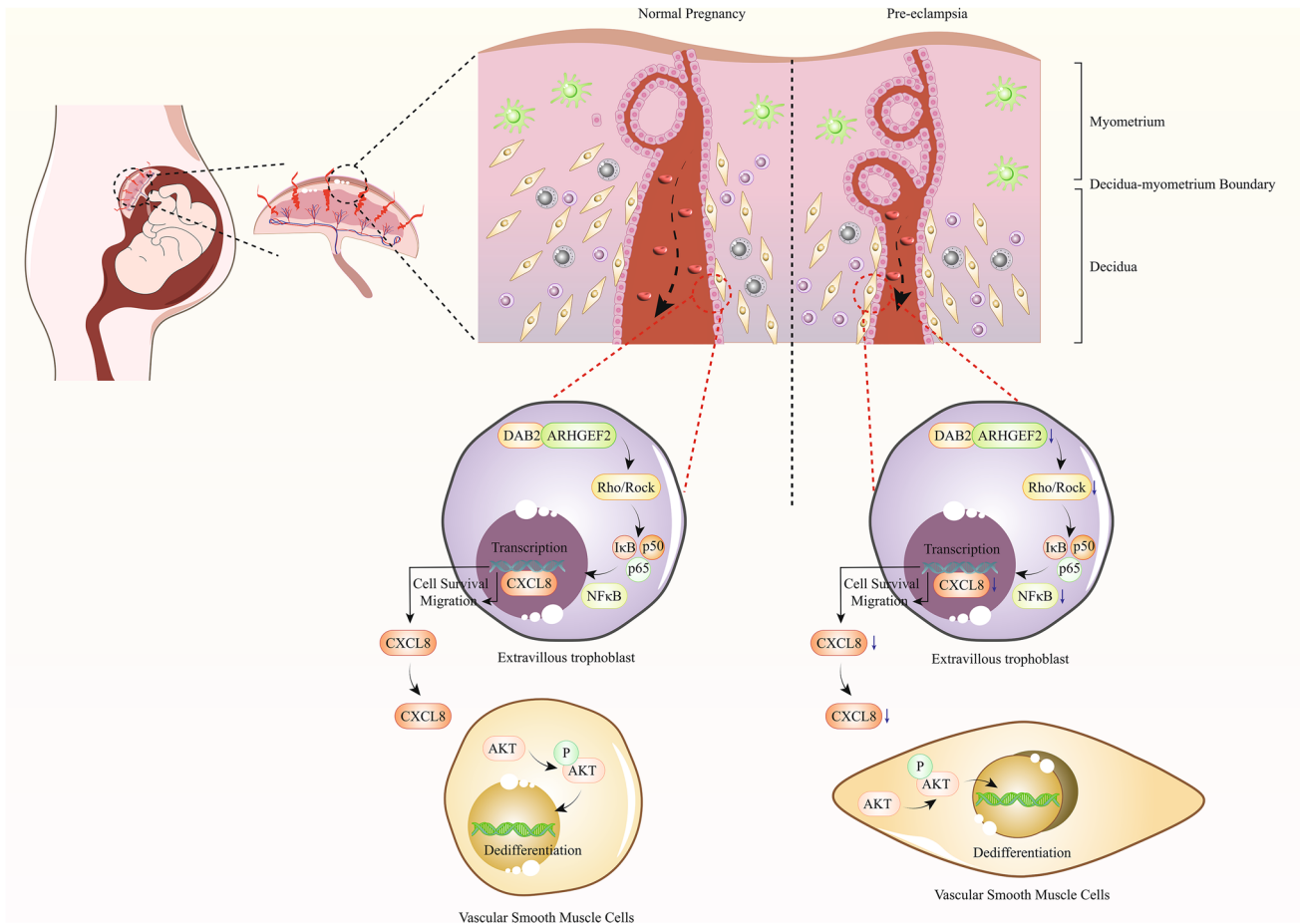
✉ Dunjin Chen
dunjinch@163.com

✉ Jingsi Chen
ceasawchen@gzhmu.edu.cn

¹ Department of Obstetrics and Gynecology, Guangdong Provincial Key Laboratory of Major Obstetric Diseases; Guangdong Provincial Clinical Research Center for Obstetrics and Gynecology; Guangdong-Hong Kong-Macao Greater Bay Area Higher Education Joint Laboratory of Maternal-Fetal Medicine; The Third Affiliated Hospital of Guangzhou Medical University, Guangzhou 510150, China

² Department of Fetal Medicine and Prenatal Diagnosis, The Third Affiliated Hospital of Guangzhou Medical University, Guangzhou 510150, China

Graphical abstract



Keywords Early-onset preeclampsia · DAB2 · CXCL8 · Spiral artery remodeling

Introduction

Preeclampsia, new-onset hypertension and proteinuria develop after 20 weeks of pregnancy and resolve after delivery [1]. This condition is characterized by maternal systemic inflammation and vascular dysfunction [2]. Early-onset preeclampsia (EOPE) is diagnosed before the 34th week of gestation [3], and often results from placental factors such as trophoblast invasion failure, endothelial dysfunction, inadequate angiogenesis, and insufficient uterine artery remodeling [4–7]. EOPE is characterized by early gestational age at onset and severe clinical symptoms. Organ damage in mothers can lead to various complications, including renal failure, HELLP syndrome (characterized by hemolysis, elevated liver enzymes, and low platelet count), thrombocytopenia, disseminated intravascular coagulation, pulmonary edema, and eclampsia (seizures). Adverse outcomes for fetuses or neonates can arise from intrauterine growth restriction (IUGR), prematurity, or placental abruption [8].

EOPE is associated with increased risks of neonatal mortality and maternal morbidity [4, 9]. Therefore, understanding the underlying mechanisms of EOPE is crucial for mitigating its pathogenesis and exploring interventions for this disease. The success of a pregnancy relies on intricate cellular interactions at the maternal–fetal interface, where spiral artery remodeling (SAR) is crucial for fetal development. Interestingly, while vessel remodeling is pathological in cardiovascular diseases such as atherosclerosis, in pregnancy, it is a highly regulated physiological process. Optimal physiological vascular remodeling involves fetal extravillous trophoblasts (EVTs) [10], yet the cellular and molecular aspects of spiral artery (SpA) remodeling have not been fully elucidated. Notably, the observed dedifferentiation, migration, and apoptosis of vascular smooth muscle cells (VSMCs) around EVT-associated vessels are hallmarks of early SpA remodeling [11]. VSMCs are not mere spectators of the remodeling process. Interactions with trophoblasts influence a range of cellular activities, including protease production

[12], cell motility [13], adhesion [14], and cytokine production [15]. The transition of vascular smooth muscle cell (VSMC) phenotypes is facilitated by various angiogenic growth factors, the most extensively researched of which are transforming growth factor (TGF) β 1 [16] and platelet-derived growth factor type BB (PDGF-BB) [17]. Unfortunately, due to material and ethical constraints, prior studies have focused mostly on histological evidence of spiral artery remodeling [18, 19]. Although the connection between insufficient remodeling of spiral arteries and obstetric complications has been known for more than four decades, our understanding of the cellular and molecular factors governing the intricate steps of this process is limited. While some headway has been achieved in recent years, further investigations are essential to gain a comprehensive understanding before viable therapeutic interventions can be developed. Here, we used single-cell RNA sequencing (scRNA-seq) of placental tissue to explore the mechanism of action between EVT and dVSMCs in spiral artery remodeling.

Our study utilized single-cell RNA sequencing (scRNA-seq) to profile placental tissues from patients with very early-onset preeclampsia (EOPE, terminated before 28 weeks) and compared them with those of matched controls. Interestingly, the identification of differentially expressed genes (DEGs) in the EVTs via scRNA-seq revealed the involvement of Disabled-2 (DAB2) in cell communication, adhesion, and multicellular processes. DAB2, which has polypyrimidine tract-binding (PTB) domains and a proline-rich domain (PRD), plays a role in growth factor signaling, cytoskeletal reorganization, and cellular adhesion [20–22]. Originally identified in ovarian tumors [23], DAB2 has also been detected in various other tumor types [24–26]. Moreover, studies indicate that chemokines and their receptors play crucial roles in SpA regulation surrounding EVTs and the maternal–fetal microenvironment [27]. The regulation of trophoblast invasion and differentiation by the chemokine-CCR1 system is considered a key molecular mechanism of maternal vascular remodeling during early pregnancy in humans [28]. However, few reports have investigated whether the chemokine system is involved in the reprogramming of vascular smooth muscle cells and the vascular remodeling process. We investigated the influence of DAB2 on trophoblast function, its potential effects on VSMCs, and the underlying regulatory mechanisms involved.

Materials and methods

This study was approved by the ethics review board of the Third Affiliated Hospital of Guangzhou Medical University. A detailed Materials and Methods section is available in the Supplemental Materials and Methods.

Results

Molecular analysis of EOPE and control placentas via single-cell RNA sequencing

To elucidate the molecular shifts at the maternal–fetal interface during midgestation in EOPE, we conducted scRNA-seq on placental tissues using the 10X Genomics platform. (Fig. 1a). After stringent quality control and doublet removal, we divided 27,330 high-quality cells into 25 unique subsets and visualized them via uniform manifold approximation and projection (UMAP) (Fig. 1b). The cell subsets of trophoblasts (including villous cytotrophoblasts [VCT1, VCT2 and VCT3]; presyncytiotrophoblasts [preSCTs]; syncytiotrophoblasts [SCTs]; extravillous trophoblasts [EVTs]; macrophages [dM1, dM2, and M3]; fetal macrophages [Hofbauer cells; HBs]; T cells; B cells; endothelial cells [Endo, Endo Lym]; epithelial cells [Epis]; cycling cells [Cyclings]; plasma cells [NK1, NK2, and CD16 NK]; decidual stromal cells [dS1 and dS2]; perivascular cells [PVs, classified in our study based on markers of vascular smooth muscle cells]; and fibroblasts [F1 and F2]) were identified based on the expression of well-defined marker genes (Fig. 1c, d).

Interestingly, Gene Ontology (GO) analysis of the DEGs downregulated in EVTs revealed three biological processes, cell communication, multicellular organization, and cell adhesion, which are related to the function of EVTs in the maternal–fetal interface (Fig. 1e). After assessing the related gene functions, we focused on DAB2, which was previously described as particularly intriguing (Fig. 1f). Moreover, Kyoto encyclopedia of genes and genomes (KEGG) analysis revealed enrichment of the PI3K-AKT pathway, MAPK pathway, hypoxia-inducible factor-1 (HIF-1) signaling pathway and other pathways in the VSMCs compared with those in the control group (Fig. 1g). This process involves the isolation of vascular smooth muscle cells (VSMC), degradation of the extracellular matrix (ECM) within the vascular wall, expansion of the blood vessel, transformation of the VSMC phenotype, migration away from the vascular wall, and subsequent apoptosis, leading to eventual removal by phagocytic macrophages [29]. Kaimoto et al. reported that the phosphatidylinositol 3-kinase/Akt signaling pathway was participated in regulating the dedifferentiation of VSMCs [30]. A study reported that PDGF-BB could increased rat aortic smooth muscle cells migration through the MAPK pathway shn [31]. Moreover, HIF-1 plays an important role in stress-responsive gene expression and is related to a number of stress factors, including metabolic stress, growth factors, and molecules present in the extracellular matrix (ECM) [32]. And KEGG pathway showed that might involved in spiral artery remodeling.

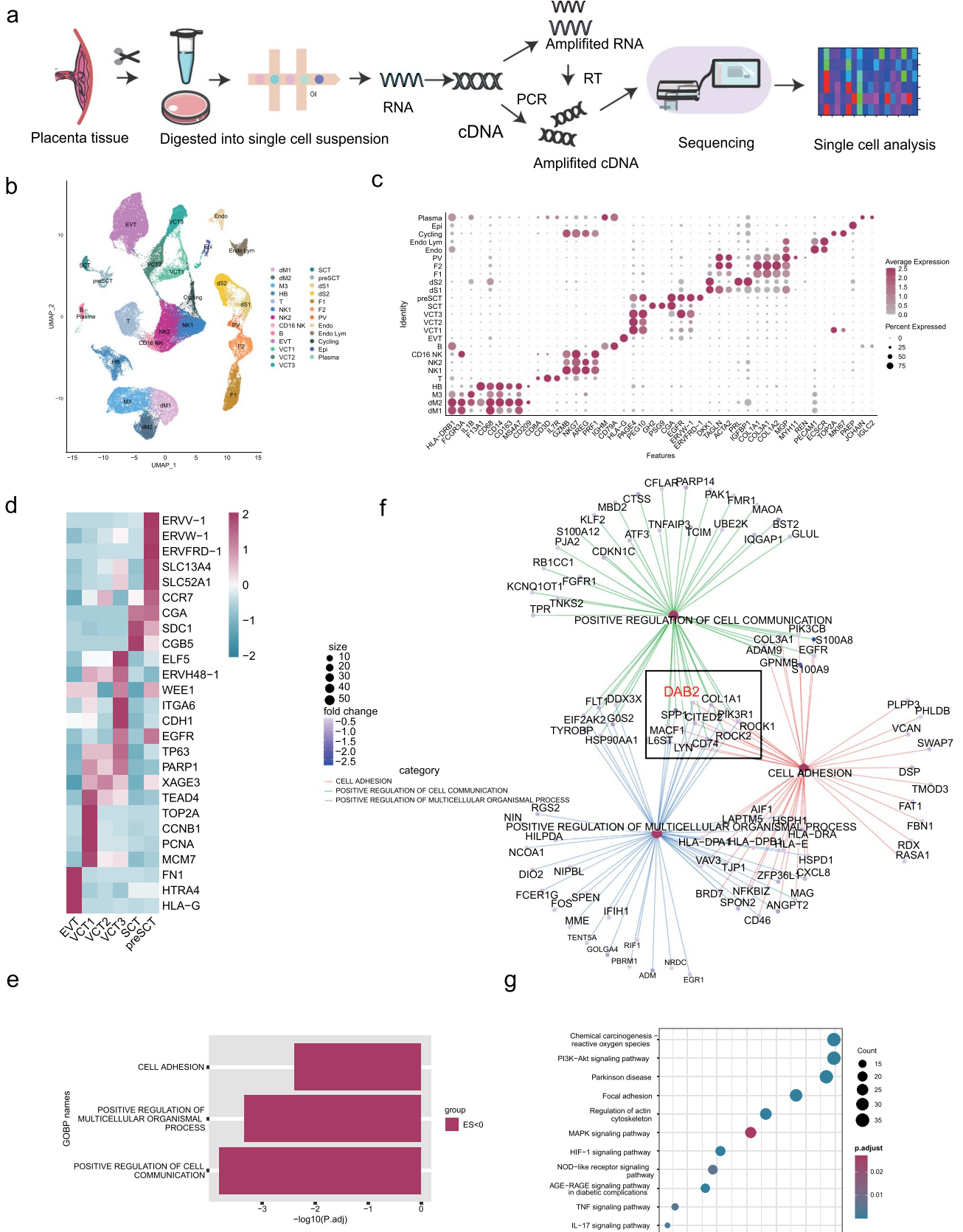


Fig. 1 Single-Cell RNA Sequencing Analysis of EOPE Compared with Matched Control Gestation. **a** A schematic representation of the single-cell RNA sequencing analysis conducted on the placenta from EOPE and its corresponding control gestation. **b** A Uniform Manifold Approximation Plot (UMAP) showcasing individual cells, each distinguished by its specific cell type through unique coloring. **c** Dot plots illustrating the expression levels of recognized lineage markers in conjunction with co-expressed lineage-specific genes. **d** A heatmap that delineates the marker genes present across different trophoblast categories, encompassing EVT, VCT1s, VCT2, VCT3, SCT, and preSCT. **e** Go-biological analysis of DEGs-downregulated in EVTs picked up the cell communication, multicellular organismal, and cell adhesion three biological processes. **f** The major enriched genes in three biological signaling functions in Fig. 1e. DAB2 was picked up for further research. **g** The enriched KEGG pathways of the DEGs-downregulated in VSMCs of EOPE compared with matched control gestation

DAB2 localization and expression in villous and decidua basalis tissues in early pregnancy

Using immunohistochemistry and immunofluorescence, we evaluated the presence of DAB2 in early pregnancy tissues. DAB2 was abundantly expressed in various trophoblasts and was present in decidual extravillous trophoblasts (the green fluorescence indicates DAB2 and KRT7, and the red fluorescence represents EVT + cells in the decidua; Fig. 2a, b). KRT7 + cells were EVT +, and the results showed that DAB2 + cells had greater fluorescence intensity in the NC group than in the EOPE group (Fig. 2c, $p^{**} < 0.01$). The transcript levels of DAB2 correlated with increasing levels of human leukocyte antigen G (HLA-G) in lysates from decidual basalis tissues collected during the first, middle

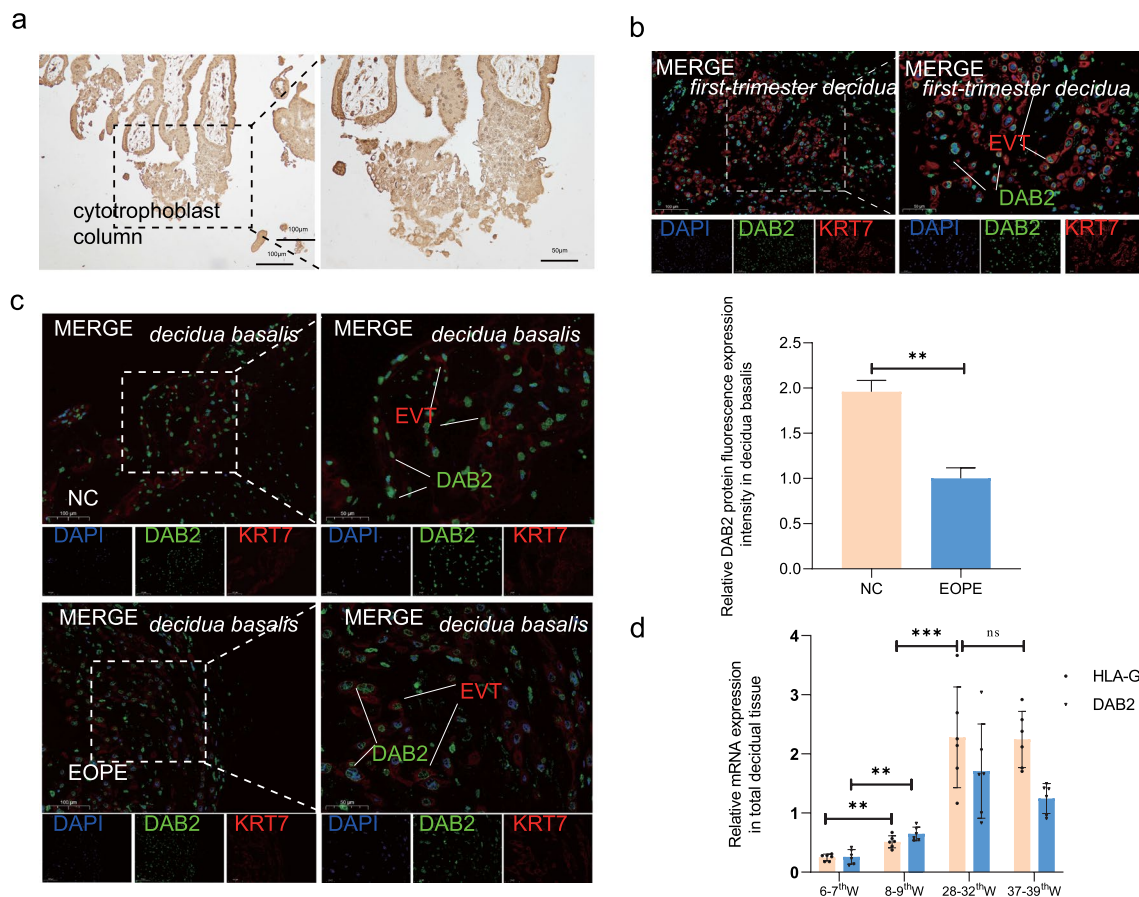
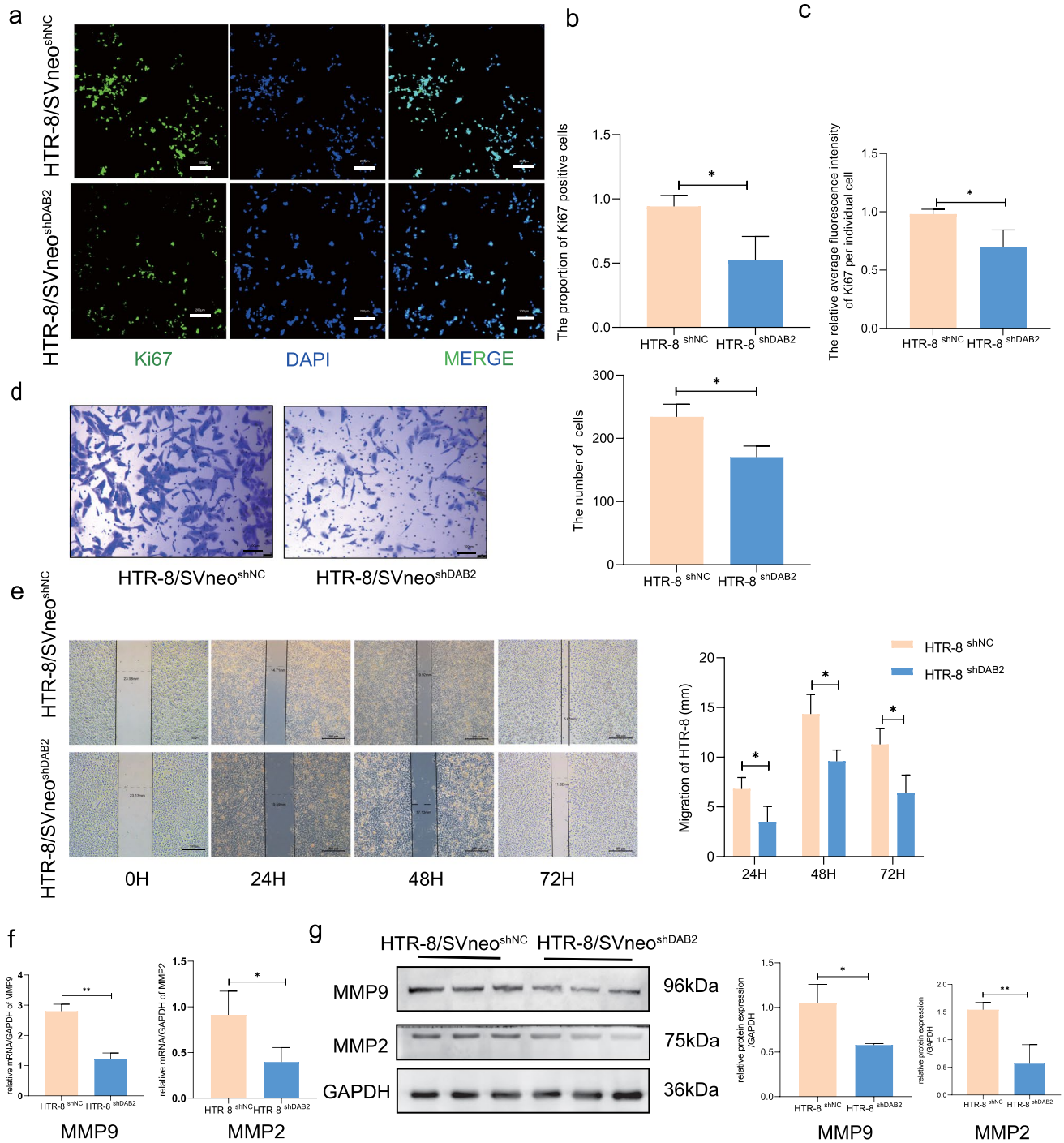


Fig. 2 Localization and Expression of DAB2 in First-Trimester Villi, Early-Onset Preeclamptic, and Control Group decidua basalis. **a** DAB2 is localized in the cytotrophoblast column of first-trimester villi. The brown signal denotes a positive DAB2 expression at this location (bar=100 µm, 50 µm), n=6. **b** KRT7 marks the extravillous trophoblast cells in decidua. DAB2, indicated by the green fluorescence, is localized within the cytoplasm of extravillous trophoblast cells in first-trimester decidua (bar=100 µm, 50 µm), n=6. **c** Immunofluorescence (IF) was utilized to compare the DAB2 expression between

EOPE and gestational-matched normal pregnant decidua basalis. The results revealed a weaker fluorescence intensity in the EOPE group compared to the control group (NC vs EOPE: 1.734 ± 0.27 vs 1.064 ± 0.26 , $p^{**} < 0.01$). This suggests a down-regulation of DAB2 expression in the EVT of the EOPE group (bar=100 µm, 50 µm), n=6. **d** qRT-PCR analysis of DAB2 and HLA-G mRNA expression in lysates from decidua basalis tissues from 6–7th week, 8–9th week, 28–32th week to 37–39th week, n=6. Above all each bar represents the mean ± SD, n=6



and late trimesters (Fig. 1d). DAB2 expression increased from the first trimester to the second trimester but remained unchanged in the third trimester (the sample information is shown in Supplementary Table S2d). During the transition from the first to the second trimester of pregnancy, important events involving vascular remodeling occur, involving a range of molecular functions.

DAB2 has a positive effect on HTR-8/SVneo cell survival and migration

Given the diminished DAB2 expression in EVTs in EOPE decidual basalis, we investigated its impact on trophoblast cell behavior using the HTR-8/SVneo cell line. DAB2 was expressed in the HTR-8/SVneo cell cytoplasm (Fig. S1a),

Fig. 3 Knockdown of DAB2 Impedes Survival and Migration Functions of HTR-8/SVneo Cells. **a** Ki67 staining assay was used to detect the survival of HTR-8/SVneo cells. The HTR-8/SVneo^{shNC} group exhibited denser green fluorescence than the HTR-8/SVneo^{shDAB2} group, indicating that DAB2 knockdown diminishes HTR-8/SVneo proliferation. **b** The proportion of Ki67-positive HTR-8/SVneo cells (HTR-8/SVneo^{shNC} vs HTR-8/SVneo^{shDAB2}: 0.94 ± 0.09 vs 0.52 ± 0.19 , $p^* < 0.05$), $n = 3$. **c** The relative average fluorescence intensity of Ki67 per individual HTR-8/SVneo cells (HTR-8/SVneo^{shNC} vs HTR-8/SVneo^{shDAB2}: 0.98 ± 0.04 vs 0.70 ± 0.15), $n = 3$. **d** Transwell assay was used to detect the cell migration. HTR-8/SVneo^{shNC} group displayed a higher count of migrated cells than HTR-8/SVneo^{shDAB2} group (HTR-8/SVneo^{shNC} vs HTR-8/SVneo^{shDAB2}: 234 ± 20 vs 170.3 ± 17.56 , bar = 200 μm , $p^* < 0.05$). **e** The scratch assay was performed to track cell migration over intervals of 24, 48, and 72 h. HTR-8/SVneo^{shNC} group consistently exhibited greater migration distances than HTR-8/SVneo^{shDAB2} group in 24, 48 and 72 h, suggesting DAB2's role in enhancing HTR-8/SVneo cell migration (HTR-8/SVneo^{shNC} vs HTR-8/SVneo^{shDAB2}: 24H: 5.117 ± 1.355 vs 3.947 ± 0.684 ; 48H: 9.58 ± 1.012 vs 6.3 ± 1.72 ; 72H: 13.037 ± 2.16 vs 9.86 ± 0.931 , bar = 200 μm , all $p^{**} < 0.01$). **f** qRT-PCR showed that the mRNA level of MMP2 and MMP9 expression were decreased in HTR-8/SVneo^{shDAB2} group (mRNA level: HTR-8/SVneo^{shNC} vs HTR-8/SVneo^{shDAB2}: MMP2: 0.91 ± 0.3 vs 0.4 ± 0.16 , $p^* < 0.05$; MMP9: 2.80 ± 0.23 vs 1.22 ± 0.20 , $p^{**} < 0.01$). **g** Western blotting (WB) showed that the protein level of MMP2 and MMP9 expression were decreased in HTR-8/SVneo^{shDAB2} group (protein level: HTR-8/SVneo^{shNC} vs HTR-8/SVneo^{shDAB2}: MMP2: 1.55 ± 0.13 vs 0.4 ± 0.16 , $p^* < 0.05$; MMP9: 1.05 ± 0.21 vs 0.58 ± 0.02 , $p^{**} < 0.01$)

and then, we transfected HTR-8/SVneo cells with siRNAs (GenePharma, Suzhou, China), especially those targeting DAB2. The transfection efficiency was confirmed by quantitative real-time polymerase chain reaction (qRT-PCR) (Fig. S1b) and western blotting (WB) (Fig. S1c). Furthermore, HTR-8/SVneo cells were transfected with lentivirus (shRNA, siRNA#1) containing mCherry (Fig. S1d), and the transfection efficiency was also measured by qRT-PCR and WB (Fig. S1e). The Ki67 staining results showed that knockdown of DAB2 suppressed HTR-8/SVneo cell viability (Fig. 3a). Transwell assays also revealed that migration was impaired after DAB2 was downregulated (Fig. 3d). A scratch assay (Fig. 3e) showed that the migration distance of the HTR-8/SVneo^{shDAB2} cells was shorter than that of the HTR-8/SVneo^{shNC} cells at the 24 h, 48 h and 72 h time points [Fig. 3c, $p^{**} < 0.01$ (24 h, 48 h, 72 h)]. Furthermore, the expression of the associated molecular markers matrix metalloproteinase 2 and 9 (MMP2 and MMP9; Fig. 3f, g) was decreased in the downregulated group, suggesting that DAB2 could enhance HTR-8/SVneo cell survival and migration, potentially influencing vascular modifications in the spiral artery.

Influence of EVT on hVSMC dedifferentiation

The phenotypic transition of VSMCs in response to environmental changes has been documented [33]. Within 6–10 gestational weeks, human decidua basalis was subjected to immunofluorescence analysis for CD31 and α -SMA in

adjacent sections to identify endothelial cells and dVSMCs, respectively (Fig. S2a). The distribution of VSMCs allowed the identification of SPAs at different stages: unremodeled (Un-Rem), early remodeling (Early-Rem), secondary remodeling (Sec-Rem), and fully remodeled (Fully-Rem) (Fig. S2a). At the Un-Rem stage, a subset of dVSMCs exhibited morphological changes, such as misalignment and a rounder shape, albeit at a relatively low frequency. During the Early-Rem stage, the multilayered VSMCs surrounding these SPAs notably appeared looser and more separated, with a substantial number displaying misalignment and a rounder morphology. As the SPAs progressed to the Sec-Rem stage, the vasculature gradually disintegrated, leading to thinner vessel walls. In the Fully-Rem vessels, α -SMA and CD31 staining was barely detectable.

To examine the impact of EVTs on SPA VSMCs, we used a human aorta VSMC (hVSMC) cell line as a model. The hVSMC were subjected to 48 h of treatment with conditional medium (48 h culture supernatant from HTR-8/SVneo cells) and complete culture medium (DMEM + 10% FBS). Morphologically, immunofluorescence staining for α -SMA indicated a notable reduction in the number of α -SMA-positive cells and an increase in the number of rounded cells, suggesting that, compared with those in complete culture medium, the hVSMCs treated with CM-HTR-8-SVneo-treated cells underwent a transition to a synthetic phenotype (Fig. S3a). Additionally, qRT-PCR and western blotting demonstrated significantly reduced expression levels of contractile markers (α -SMA, SM22 α , calponin, and MYH-11) and protein levels (α -SMA and MYH11) in CM-HTR-8/SVneo-treated cells (Fig. S3b, c, $p^{**} < 0.01$). According to prior research, VSMCs with a synthetic phenotype tend to migrate away from blood vessels and undergo apoptosis [34]. The protein levels of MMP2 and MMP9 were elevated in the HTR-8/SVneo culture medium treatment group (Fig. S3e, $p^{**} < 0.01$ (MMP9), $p^* < 0.05$ (MMP2)). A greater proportion of cells underwent apoptosis in the HTR-8/SVneo cell supernatant than in the control supernatant (Fig. S3f). Furthermore, 48-h supernatants from villous explants revealed decreased transcriptional levels of cell differentiation markers following 48 h of coculture with VSMCs, suggesting reduced cell differentiation in the CM-villous explant group (Fig. S3g, $p^{**} < 0.01$, $p^* < 0.05$). Based on our results, trophoblast cells can induce dedifferentiation in hVSMCs, promoting migratory and apoptotic processes that contribute to the remodeling of spiral arteries.

DAB2 has a positive influence on HTR-8/SVneo-mediated hVSMC reprogramming

The positive influence of DAB2 on trophoblast survival and migration and the function of DAB2 in trophoblast

cells on the vascular smooth muscle of the decidual spiral artery need further discussion. After 48 h, the culture media of HTR-8/SVneo^{shDAB2} and HTR-8/SVneo^{shNC} cells were collected and then added to hVSMCs (the hV^{+H8shNC} and hV^{+H8shDAB2} groups, respectively). The cells became round, which indicated that the hVSMCs in the hV^{+H8shNC} group might have adopted a synthetic phenotype compared with those in the hV^{+H8shDAB2} group (Fig. 4a, white arrow). The qRT-PCR and western blotting results revealed that the transcription levels of contractional markers (Fig. 4b, $p^* < 0.05$) and proteins (Fig. 4c, $p^* < 0.05$) were significantly lower in the CM-HTR-8/SVneo^{shNC}-treated cells than in the CM-HTR-8/SVneo^{shDAB2}-treated cells.

A villous and decidua coculture system [35] was used to investigate the effect of conditioned medium-induced spiral artery remodeling (Fig. 4e). In the control group, decidua tissue without conditioned medium was collected, and the blood vessels exhibited complete morphology and no obvious signs of remodeling. Compared to those in the hV^{+H8shNC} group, the hV^{+H8shDAB2} group had fewer remodeled arteries, which were characterized by dVSMC layers (the green fluorescence represents α -SMA-positive cells) (Fig. 4f). dVSMC disruption and clear morphologic vascular remodeling changes, including disintegration of the dVSMC layers and a larger vascular lumen, were observed in the hV^{+H8shNC} group (white arrow). The proportion of vascular remodeling in each group was measured. We defined the phenomenon of vascular migration outside the vessel site as the remodeling group, and the other group was defined as the nonremodel group. The visual field where vascular remodeling occurred was selected, and five films were taken for quantitative analysis according to the number and proportion of vascular remodeling events. The results showed that the proportion of vascular remodeling was 64.7% in the hV^{+H8shNC} group and 40.3% in the hV^{+H8shDAB2} group, with a significant difference between the two groups ($p^* < 0.05$).

Similarly, after 48 h of treatment, the supernatant of HTR-8/SVneo cells was collected from which DAB2 was knocked down, after which the 24-h migration ability was weaker than that of the NC group, and the number of apoptotic cells was less than that of the NC group (Fig. S4a, b, c).

Elucidation of target genes and mediators influencing HTR-8/SVneo and hVSMC reprogramming

We conducted an RNA-seq transcriptomic analysis of HTR-8/SVneo cells and hVSMC to discern the transcriptional changes in trophoblast cells after DAB2 knockdown and to pinpoint the mediators responsible for hVSMC reprogramming. A comparison revealed 2199 downregulated genes and 3317 upregulated genes that were significantly

altered > 1.5-fold in the HTR-8/SVneo^{shDAB2} population compared with the HTR-8/SVneo^{shNC} population (p value < 0.05; Fig. S5a). We overlapped the DEGs identified via RNA-seq with the EVT DEGs from single-cell sequence data to obtain 227 genes that were involved in the PI3K-AKT pathway and the IL-17 signaling pathway, which are involved in cell migration and cell survival (Fig. 5a). Most of the pathways were associated with cell migration regulation and the insulin-like growth factor receptor signaling pathway, which could explain why the function of HTR-8/SVneo cells changed after DAB2 was knocked down (Fig. 5b). Interestingly, chemokines, known for recruiting leukocytes, are highly expressed at the maternal–fetal interface. In addition to immune cells, trophoblast cells are also involved in chemokine regulation [27].

We selected the top ten differentially expressed chemokines and inflammatory factors and verified the mRNA levels through qRT-PCR (Fig. 5d). We also reviewed the relevant literature to identify the genes related to cell migration and various ontologies related to signaling and some vascular processes. Finally, the feasible target genes were identified as CXCL8, CXCL1, and IL6 because of their differential expression and relative expression. The concentration in the supernatant was subsequently verified via ELISAs (Elisa Kit, ABclonal, Wuhan, China). Compared with CXCL1 and IL-6, CXCL8 exhibited the most significant difference in expression between the two groups of supernatants (Fig. 6a). CXCL8 was selected as a mediator that might mediate dVSMC reprogramming.

For hVSMC, we analyzed the transcriptional shifts triggered by trophoblast 48-h HTR-8/SVneo-conditioned medium, and there were significant changes in gene expression. Specifically, in the hV^{+H8shDAB2} group, 398 genes were significantly suppressed, whereas 154 genes were upregulated with 1.5-fold changes ($*p$ value < 0.05; Fig. S5c). After the DEGs identified from the hVSMC RNA sequencing and PV scRNA-seq data were overlapped, KEGG analysis revealed enrichment of genes related to cytokine–cytokine receptor interactions, the ECM-receptor pathway, and the NOD-like receptor signaling pathway, which are related to the tissue remodeling process (Fig. 5e). GSEA KEGG analysis revealed that the IL8/CXCR1/2 pathway was suppressed in the EOPE group (Fig. 5f). According to the enrichment analysis of downregulated DEGs in EOPE in PV, the main enriched pathways included those involved in the regulation of cell differentiation, response to cytokines and apoptotic processes (Fig. S5e, f), which was also consistent with the hypothesis that in PE, spiral artery remodeling was impaired, smooth muscle cells were poorly responsive to chemokines, the dedifferentiation process was inhibited, and the dVSMC apoptotic process was reduced.

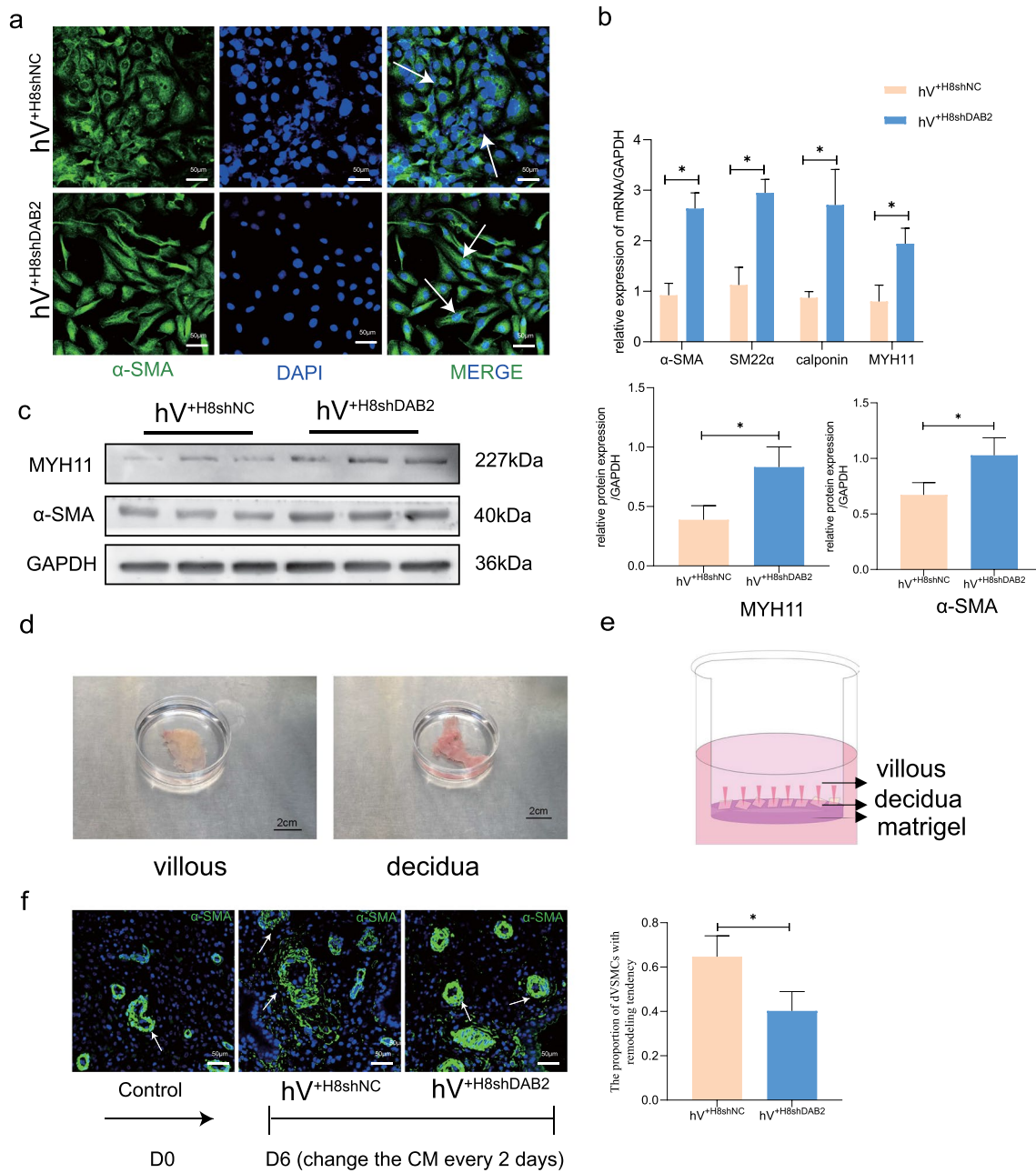


Fig. 4 DAB2 in HTR-8/SVneo Facilitates hVSMCs Phenotypic Transition and Modulates SPA Remodeling. **a** Cell immunofluorescent staining of α -SMA in hVSMCs, which treated with the different group CM-HTR-8/SVneo ($hV^{+H8shNC}$ group and $hV^{+H8shDAB2}$ group), for investigate the effect of DAB2 differences in trophoblast cells on hVSMCs. The cells in $hV^{+H8shDAB2}$ group remain hold the spindle shape, and the $hV^{+H8shNC}$ group turned to round shape, as the white arrows indicated. bar = 200 μ m. **b** The relative mRNA level (calponin, MYH-11, α -SMA and SM22 α) were detected by qRT-PCR. The contractile indicators in $hV^{+H8shNC}$ group were lower than $hV^{+H8shDAB2}$ group, which means that the DAB2 in trophoblasts could switch hVSMCs phenotype ($hV^{+H8shNC}$ vs $hV^{+H8shDAB2}$: calponin: 0.871 ± 0.122 vs 2.7 ± 0.702 ; MYH-11: 0.797 ± 0.324 vs 1.941 ± 0.306 ; α -SMA: 0.921 ± 0.236 vs 2.638 ± 0.309 ; SM22 α : 1.125 ± 0.349 vs

2.947 ± 0.27 , all $p^* < 0.05$). **c** The relative protein level (MYH-11, α -SMA) were detected by WB. The contractile indicators in CM of HTR-8/SVneo were lower than the $hV^{+H8shDAB2}$ group ($hV^{+H8shNC}$ vs $hV^{+H8shDAB2}$: MYH-11: 0.389 ± 0.118 vs 0.8315 ± 0.098 ; α -SMA: 0.672 ± 0.11 vs 1.029 ± 0.157 , all $p^* < 0.05$). **d** Images of the villi and decidua in the first trimester. **e** Schematic representation of the PDC model system. **f** Immunofluorescent staining of the decidua tissue in co-cultured villous-decidua model with different conditioned media treatments. α -SMA-positive (green) represent the VSMC of spiral artery vascular. bar = 50 μ m. Samples were were acquired from 12 pregnant women. The statistical analysis is performed based on the record from five cases for each section and five random views in each case. The proportions of remodeling are as follows: ($hV^{+H8shNC}$ vs $hV^{+H8shDAB2}$: 0.647 ± 0.09 vs 0.403 ± 0.087 , $p^* < 0.05$)

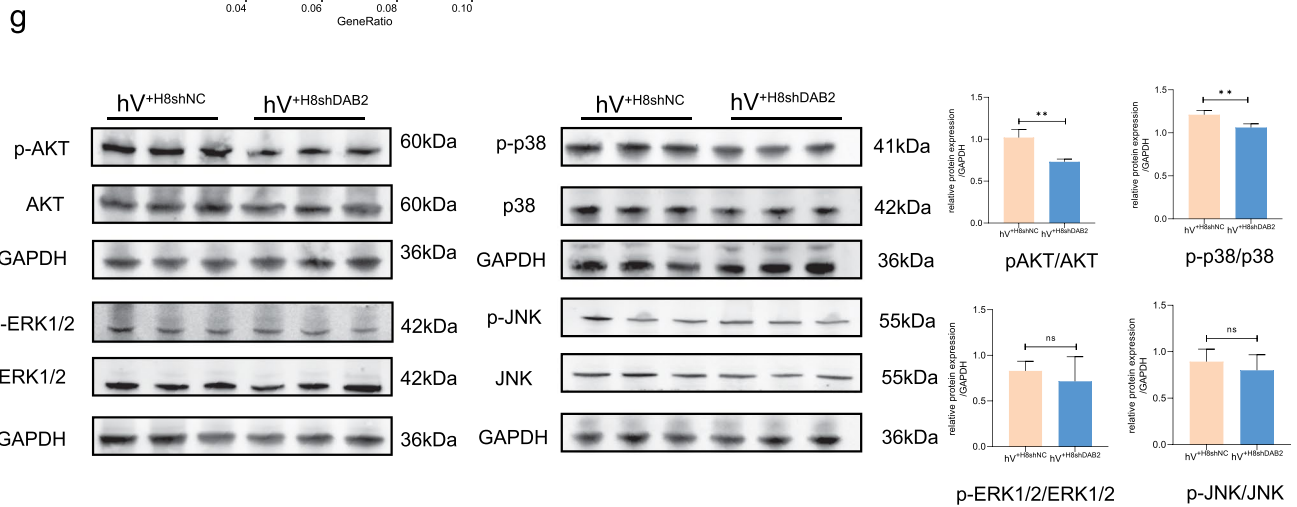
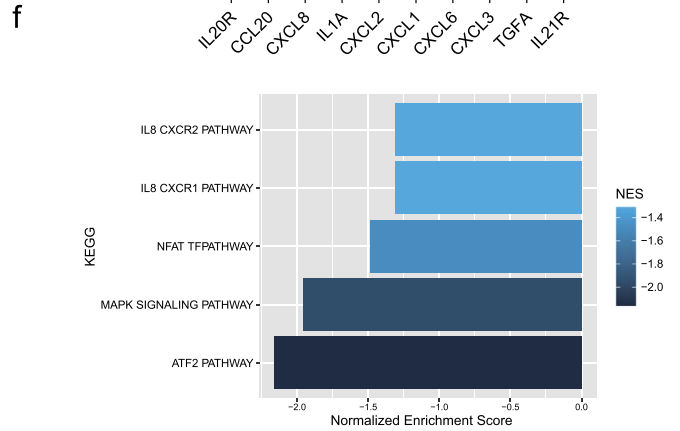
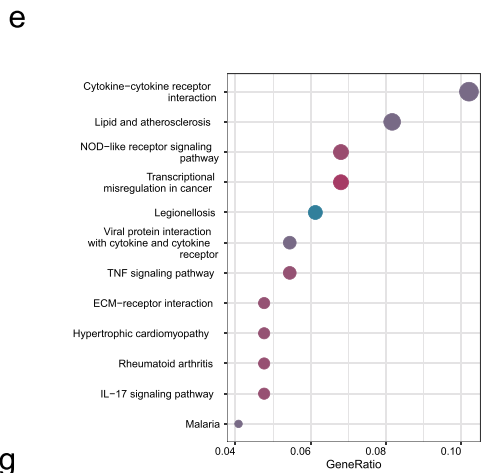
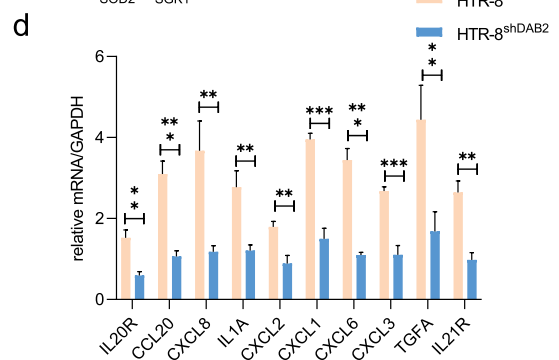
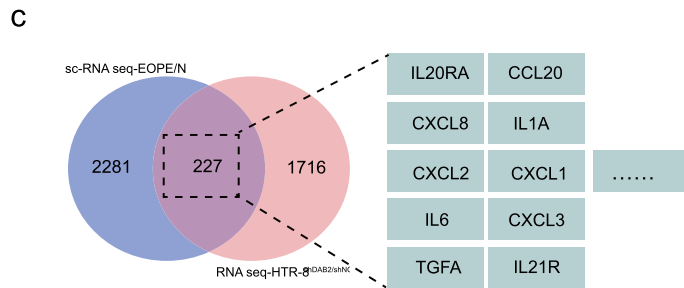
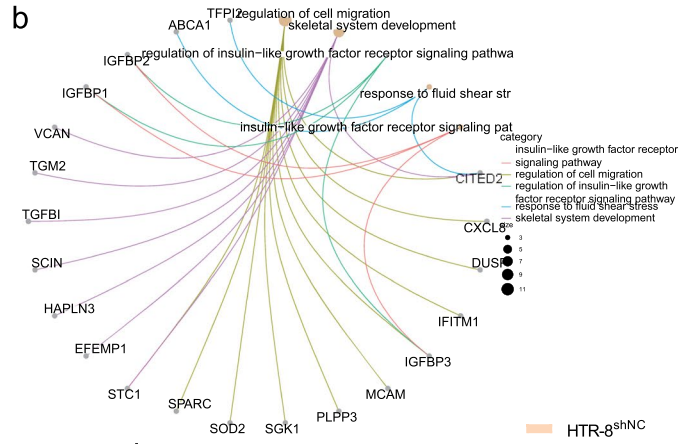
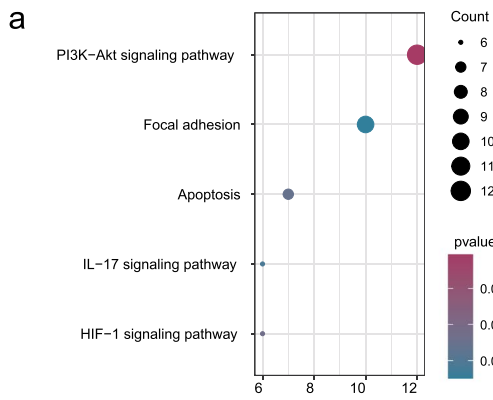


Fig. 5 Comprehensive Discovery of Target Genes Modulating HTR-8/SVneo Function and the Mediators Governing hVSMCs Reprogramming. **a** KEGG enrichment pathway analysis of the intersection gene of down regulated genes in HTR-8/SVneo^{shDAB2} group of RNAseq and EVT genes in sc-RNA seq. **b** The enrichment circle figure showed that these co-down-regulated genes were enriched in insulin-like growth factor receptor signaling pathway and other pathways, which related with the cell survival and motility. **c** Intersection of downregulated genes from HTR-8/SVneo RNA-seq and EVT from scRNA-seq. Ten distinctly different chemokines and inflammatory factors potentially involved in the regulation of the maternal–fetal interface were selected for further enrichment analysis. **d** The mRNA level of chemokine and inflammatory factors were decreased in HTR-8/SVneo^{shDAB2} group then verified by qRT-PCR. (HTR-8^{shNC} vs HTR-8^{shDAB2}: IL20R: 1.525 ± 0.193 vs 0.594 ± 0.093 ; CCL20: 3.442 ± 0.286 ; CXCL8: 3.670 ± 0.737 vs 1.177 ± 0.1521 , IL1A: 2.771 ± 0.407 vs 1.207 ± 0.143 , CXCL2: 1.795 ± 0.131 vs 0.889 ± 0.198 ; CXCL1: 3.098 ± 0.318 vs 1.062 ± 0.143 ; IL6: 3.951 ± 0.154 vs 1.498 ± 0.262 vs 1.099 ± 0.063 ; CXCL3: 2.676 ± 0.108 vs 1.105 ± 0.226 ; TGFA: 4.436 ± 0.853 vs 1.681 ± 0.486 ; IL21R: 2.641 ± 0.286 vs 0.977 ± 0.183 , $p^* < 0.05$, $p^{**} < 0.01$). **e** Go biological analysis of co-downregulated genes in hV^{+H8shDAB2} group of hVSMCs RNA seq and PV of sc-RNA seq. **f** GSEA KEGG enrichment analysis of co-down-regulated genes in hV^{+H8shDAB2} group of hVSMCs RNA seq and PV of sc-RNA seq. The enrichment analysis of GSEA KEGG signaling pathway showed that IL8 CXCR1/2 signaling pathway, and MAPK signaling pathway were down-regulated by analyzing the differential gene expression levels of co-down-regulated genes in hV^{+H8shDAB2} group of hVSMC RNA seq and PV of sc-RNA seq. **g** After hVSMC was co-cultured with medium supernatants from different groups, WB was used to detect important molecules (AKT, p-AKT, p38, p-p38, p-ERK1/2, ERK1/2, p-JNK, JNK) in both pathways. The results showed that only PI3K/AKT pathway and p-p38 MAPK pathway were significantly different (hV^{+H8shNC} vs hV^{+H8shDAB2}: p-AKT/AKT: 1.02 ± 0.09 vs 0.73 ± 0.03 , $p^{**} < 0.01$; p-p38/p38: 1.211 ± 0.05 vs 1.062 ± 0.04 , $p^* < 0.05$; p-ERK1/2/ERK1/2: 0.083 ± 0.11 vs 0.715 ± 0.27 , $p = 0.53$; p-JNK/JNK: 0.893 ± 0.14 vs 0.80 ± 0.17 , $p = 0.49$; $n = 3$)

By reviewing past research on the pathways involved in migration and phenotypic transition, we speculated that the mitogen-activated protein kinase (MAPK) [31] and PI3K/AKT [30, 36, 37] signaling pathways may play a role in mediating downstream regulatory effects. In conclusion, AKT/p-AKT, ERK/p-AKT, JNK/p-JNK, and p38/p-p38 were assessed to investigate the effects of trophoblasts on hVSMC functions (Fig. 5g). The results showed that both the PI3K/AKT and MAPK/P38 pathways were promoted after treatment of smooth muscle cells with different supernatants, but the difference in the PI3K pathway was more significant (Fig. 5g, $** p < 0.01$, $* p < 0.05$). In the next work, we examined the role of the PI3K pathway in mediating the dedifferentiation of hVSMCs.

DAB2 through CXCL8/PI3K/AKT pathway regulate hVSMC dedifferentiation

Chemokines, which are particularly vital at the maternal–fetal interface, bind to G protein-coupled receptors, subsequently activating specific signaling pathways (Fig. 6c)

[27]. The results showed that EVT cells strongly expressed CXCL8 (Fig. 6b). Exogenous recombinant CXCL8 protein (Abcam, ab259397, USA) was used to investigate the function of CXCL8. CXCL8 (10 ng/ml, according to the manual) was added to the cell culture medium for coculture for 48 h. According to the cellular immunofluorescence results, the cells changed from long fusiform to round, and the levels of MYH11 and α -SMA decreased, which indicated that CXCL8 promoted the dedifferentiation of hVSMCs (Fig. 6d, e). Furthermore, the results indicated that CXCL8 promoted hVSMC migration and apoptosis (Fig. S4d, e, f). Furthermore, CXCL8 activated the PI3K pathway, and the pAKT/AKT ratio was increased (Fig. 6f).

CXCL8 signaling plays a role mainly through two cell-surface receptors, CXCR1 and CXCR2 [38]. Navarixin (20 nM, CXCR1 and CXCR2 receptor antagonist, MCE, HY-10198, China) and a PI3K pathway inhibitor (LY29400, Selleck, S1105, USA) were used to inhibit the function of CXCL8 and the PI3K pathway to further determine whether hVSMC differentiation was due to the regulation of CXCL8 and the PI3K/AKT pathway. The cells were divided into the following groups: CM-HTR-8/SVneo^{shNC} + CXCR1/2 antagonist/LY29400, CM-HTR-8/SVneo^{shNC} + DMSO, CM-HTR-8/SVneo^{shDAB2} + CXCR1/2 antagonist/LY29400 and CM-HTR-8/SVneo^{shDAB2} + DMSO.

After the CXCR1/2 antagonist was added to CM-HTR-8/SVneo^{shNC}, the hVSMCs maintained the shape of a long spindle, and the dedifferentiation process was inhibited (Fig. 7a). Moreover, there were no significant differences among the other three groups. After the CXCR1/2 antagonist was added to the CM-HTR-8/SVneo^{shNC} group, more contractile markers were expressed than in the DMSO group (Fig. 7b). These results indicated that the CXCL8 in the supernatant might have a critical effect in the dedifferentiation process. Moreover, after CM-HTR-8/SVneo cells were treated with the CXCR1/2 antagonist, the expression of pAKT was reduced compared with that in the DMSO group. The other trend was consistent with the above result.

After incubation with LY29400, the cells in the CM-HTR-8/SVneo^{shNC} group remained spindle-shaped. The cells in the CM-HTR-8/SVneo^{shNC} + DMSO group were round (Fig. 7c). Similarly, contractile markers were detected by WB. After LY29400 was added to CM-HTR-8/SVneo^{shNC} cells, the expression of MYH11 and α -SMA was greater than that in the DMSO group (Fig. 7d). Moreover, pAKT was downregulated, but there was no significant difference between the two groups when LY29400 cells were cocultured with CM-HTR-8/SVneo^{shNC} or CM-HTR-8/SVneo^{shDAB2}.

To further verify whether CXCL8 is a mediator of dedifferentiation in hVSMC, we added exogenous CXCL8 protein to different subgroup supernatants, and cell morphological changes and the expression of differentiation factors

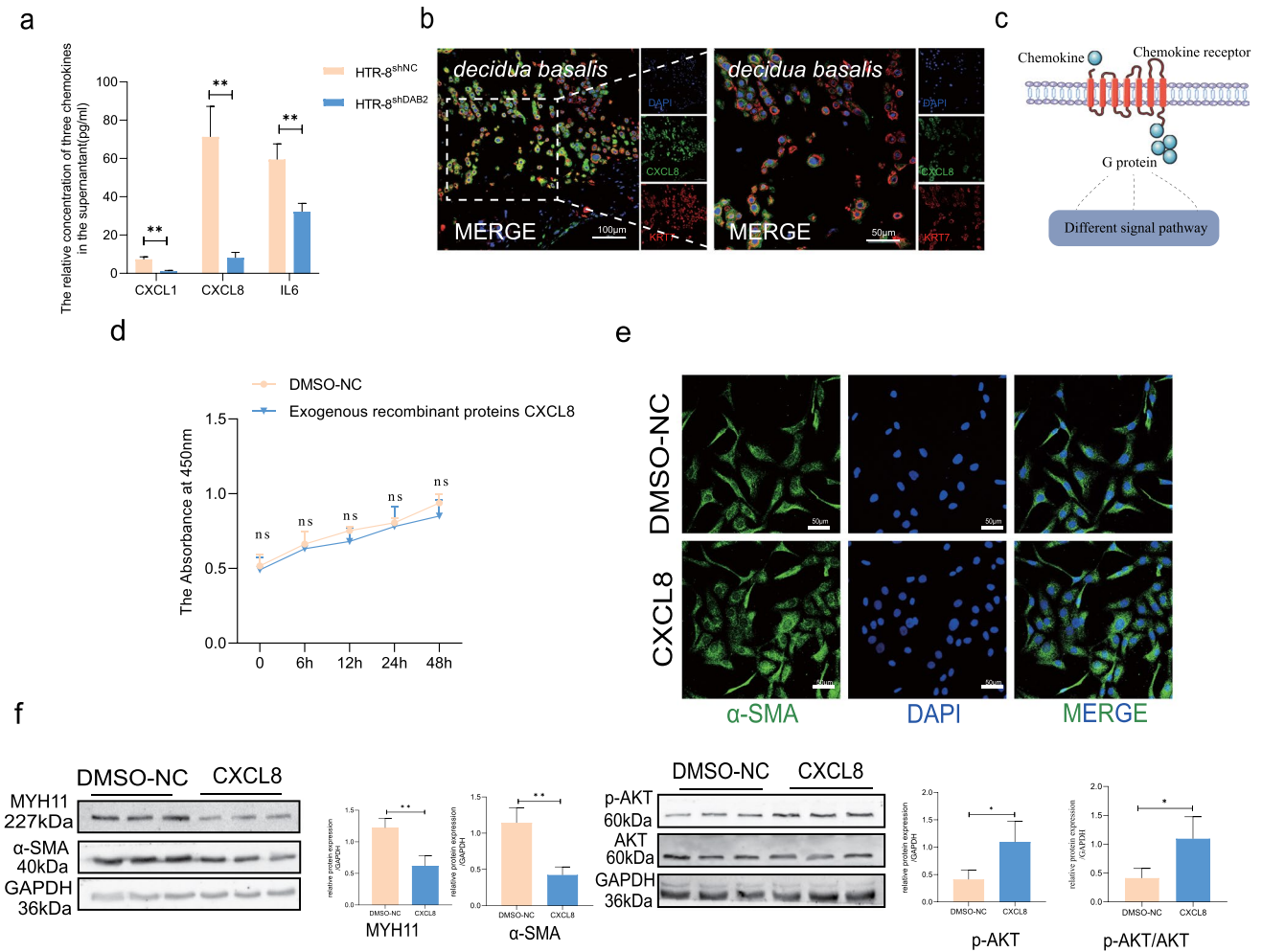


Fig. 6 CXCL8 was expressed in trophoblast and could modulate hVSMCs dedifferentiation. **a** The relative concentration of CXCL1, CXCL8 and IL-6 in supernatant of HTR-8/SVneoshNC and HTR-8/SVneoshDAB2 were detected by Elisa analysis. The relative concentration expression of CXCL1, IL-6 and CXCL8 were exhibited. (HTR-8shNC vs HTR-8shDAB2: CXCL1: 7.313 ± 1.315 vs 1.164 ± 0.417 , $p^{**} < 0.01$; CXCL8: 71.29 ± 15.9 vs 8.164 ± 2.765 , $p^{**} < 0.01$; IL6: 59.49 ± 8.166 vs 32.19 ± 4.315 , $p^{**} < 0.01$, respectively). **b** CXCL8 (The green fluorensacen) was expressed in first trimester decidua basalis and located in EVTs (KRT7⁺ represents EVT cells in decidua). **c** Schematic representation illustrating the interaction of chemokines with seven-transmembrane G-protein-coupled receptors, leading to G-protein subunit dissociation, activation of signaling pathways, and subsequent cellular function modulation. **d** CCK8 cytotoxicity assay was performed at 6 h, 12 h, 24 h and 48 h time points, and there was no significant difference between them (DMSO-NC vs CXCL8: 0 h: 0.52 ± 0.06 vs 0.49 ± 0.05 ; 6 h:

0.67 ± 0.07 vs 0.65 ± 0.06 ; 12 h: 0.74 ± 0.04 vs 0.68 ± 0.06 ; 24 h: 0.78 ± 0.06 vs 0.79 ± 0.10 ; 48 h: 0.93 ± 0.05 vs 0.88 ± 0.06 ; $p > 0.05$). $n = 6$. **e** A morphological shift towards a rounded cell shape was observed after been treated with CXCL8, whereas cells in the DMSO control group maintained a spindle shape. **f** The dedifferentiation marker (MYH-11 and α -SMA) were examined by western-blot analysis. The protein expression of MYH-11 and α -SMA were decreased (DMSO-NC vs CXCL8: MYH-11: 1.222 ± 0.151 vs 0.619 ± 0.153 , $p^{**} < 0.01$; α -SMA: 1.145 ± 0.203 vs 0.424 ± 0.111 , $p^{**} < 0.01$) when treated with exogenous recombinant protein CXCL8, which means that CXCL8 could promote hVSMCs dedifferentiation and might participate in the process of spiral artery remodeling. AKT and pAKT were important indexes in the PI3K/AKT pathway. After treatment with CXCL8, the pAKT expression was increased and indicated that CXCL8 could activate PI3K signal pathway (DMSO-NC vs CXCL8: p-AKT: 0.4129 ± 0.168 vs 1.095 ± 0.379 , $p^{*} < 0.05$; p-AKT/AKT: 0.4126 ± 0.167 vs 1.096 ± 0.379 , $p^{*} < 0.05$)

were detected to determine whether CXCL8 could rescue the process of dedifferentiation. The results showed that the cells became round after the addition of CXCL8 to the knockdown group (Fig. 7e). The results showed that CXCL8 secreted by trophoblasts was an important key factor in regulating hVSMC dedifferentiation.

Preliminary investigation of the mechanism of DAB2-mediated regulation of CXCL8

The HTR-8/SVneo RNA-seq analysis showed that the mRNA levels of CXCL8 were decreased after DAB2 was knocked down. To determine how DAB2 modulates

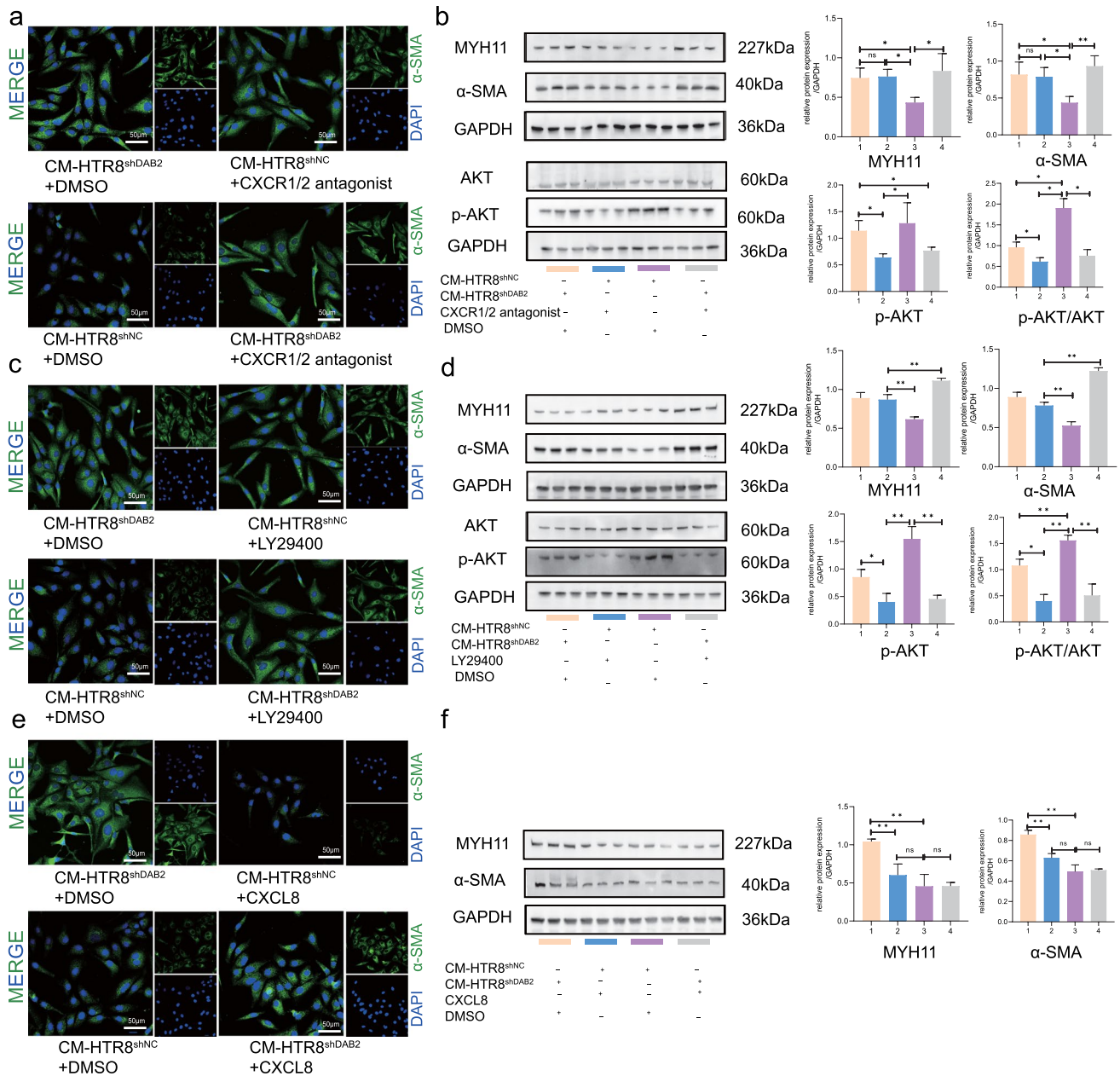
CXCL8, we employed protein mass spectrometry (MS) to identify DAB2-interacting proteins. After excluding the influence of negative controls, we identified a total of 294 proteins interacting with DAB2. GO and KEGG enrichment analyses of the molecules revealed that the signaling pathways were mainly involved in cell migration and differentiation and in the survival and migration of trophoblast cells (Fig. S6a, b). After overlapping the RNA-seq and IP-MS data, we identified Rho guanine nucleotide exchange factor 2 (GEF-H1 or ARHGEF2) (Fig. S6c, d). GEF-H1 promoted the conversion of GDP to GTP and subsequently regulated Rho-GTPases. Rho GTPases are a family of small G proteins that play major roles in cell migration and the metastatic process and participate in cellular processes that regulate the cytoskeleton [39]. The cells were divided into the input group (the HTR-8/SVneo cell protein sample), the IP-DAB2 group (the sample in which proteins that interact with DAB2 were pulled down according to the IP kit), and the IgG negative control group. The interaction of DAB2 with GEF-H1 was verified by co-IP analysis (Fig. S6g), and the GEF-H1 protein level was found to be decreased in EOPE placental tissues (Fig. S6h). Moreover, we used Genome Browser (<https://genome.ucsc.edu/>) and PROME (https://algggen.lsi.upc.es/cgi-bin/promo_v3) analyses to predict the binding factors of CXCL8, and a total of 162 transcription factors were predicted (Fig. S6e). Among the three transcription factors, NF- κ B was decreased after DAB2 was knocked down in HTR-8-SVneo cells (Fig. S6h). NF- κ B is a vital mediator of placentation and can regulate placentation through the modification of cytokine expression, as well as cell phenotype and function [40]. We hypothesized that DAB2 might interact with GEF-H1 to activate the Rho/NF- κ B pathway to regulate CXCL8 expression, which needs further validation.

Discussion

The clinical course of EOPE is highly unpredictable, and most commonly used criteria for severity, such as the magnitude of hypertension and proteinuria, are poorly associated with maternal and fetal outcomes [41, 42]. This uncertainty complicates decisions regarding the optimal timing for delivery, underscoring the need for more reliable biomarkers or molecular targets. Our study contributes to this field by revealing the potential role of Disabled-2 (DAB2) in the pathophysiology of EOPE. Remarkably, we showed that DAB2 may regulate the secretion of C-X-C motif chemokine ligand 8 (CXCL8), which subsequently activates the phosphoinositide 3-kinase/protein kinase B (PI3K/AKT) pathway in hVSMCs, as shown in Graphical abstract. This pathway is crucial for spiral artery remodeling, a key process in

placentation. Our findings not only illuminate a novel aspect of DAB2 function but also hint at its broader implications in vascular biology and preeclampsia management.

Importantly, in this study, we elucidated the role of DAB2 in modulating the function and interaction of trophoblasts and vascular smooth muscle cells (VSMCs) during spiral artery remodeling. Several studies have reported the immunomodulatory effect of DAB2, but few studies have investigated the function of trophoblast. With its multiple binding domains, DAB2 has emerged as a key orchestrator in various signaling pathways, facilitating complex protein–protein interactions [43]. Intriguingly, parallels drawn from oncological studies in which DAB2 expression was associated with tumor progression suggest that DAB2 may play a unique role in promoting cell viability and migration [44]. These cancer research findings are consistent with our observations, suggesting that DAB2 enhances EVT's ability to modify vascular structures, akin to facilitating tumor cell migration and invasion [45, 46]. When DAB2 was knockdown, we found that the dedifferentiation process of hVSMC was blocked, suggesting that DAB2 might be involved in the regulation between EVTs and dVSMCs. We validated the importance of DAB2 for VSMC dedifferentiation via placental tissue and cell models *in vitro*. At the maternal–fetal interface, chemokines, such as CXCL14, CXCL12, CCL24 and so on have been verified expressed in primary trophoblast, might regulate intercellular communication [47, 48]. Of particular interest is CXCL8, which is known to be involved in inflammation-related diseases. Ruhul H Choudhury et al. reported that the CXCL8 was secreted by EVTs and then induce endothelial cell expressed CCL14 and CXCL6 [49]. In addition, CXCL8 can induce immune cells to participate in the occurrence of vascular remodeling [50]. Moreover, CXCL8 can promote trophoblast cells migration and promote the progression of spiral artery remodeling [51]. Therefore, we investigated whether EVT-derived CXCL8 is involved in the regulation of decidual vascular smooth muscle cell dedifferentiation. After the function of CXCL8 was inhibited, the cells exhibited a long fusiform morphology, and the MYH11 and α -SMA levels did not decrease compared with those in the DMSO group. We found that there was no difference between the CM-HTR-8/SVneo^{shDAB2} and CM-HTR-8/SVneo^{shNC} added with the CXCR1/2 group, which indicates that CXCL8 plays an irreplaceable role in regulating hVSMC dedifferentiation and there are other factors that regulate the PI3K signaling pathway. Moreover, the addition of exogenous CXCL8 to the DAB2 knockdown group supernatant rescued the abnormal dedifferentiation of hVSMC. However, pAKT expression differed between the CM-HTR-8/SVneo^{shDAB2} group and the CM-HTR-8/SVneo^{shNC} with the CXCR1/2 group, indicating that other cytokines, except CXCL8, activate the PI3K pathway. A study on asthma revealed that activating the PI3K/



AKT signaling pathway could promote the migration and proliferation of hVSMC [52]. Additionally, PDGF- β could activate phosphorylation of Akt and induce proliferation and migration of VSMCs [53]. When the PI3K inhibitor LY29400 was added to the supernatant of HTR-8/SVneo^{shNC} cells, the expression of p-AKT decreased, the cell morphology also remained long and fusiform, and the contractile indices did not decrease. It indicated that PI3K pathway plays an important role in hVSMC dedifferentiation and could broaden our understanding.

Furthermore, our IP-MS findings indicated an interaction between DAB2 and GEF-H1, as verified by co-IP analysis. GEF-H1 is implicated in several cellular processes, from

barrier permeability to cancer [54]. Notably, Rho GTPases, which are pivotal for cell migration and cancer metastasis, may also influence the tumor microenvironment and inflammation [39]. NF- κ B is a vital mediator of placental inflammation [40] and a transcription factor of CXCL8 [55, 56]. These findings link DAB2's function to broader cellular processes such as cell migration and inflammation, further emphasizing its potential as a therapeutic target in managing disorders related to placental insufficiency.

While our study provides important insights into the role of DAB2 in spiral artery remodeling and its broader implications in EOPE, there are certain limitations, and further research is needed. One of the primary limitations is the

Fig. 7 DAB2 in EVT mediated CXCL8/PI3K/AKT pathway regulating hVSMC dedifferentiation. **a** Cell immunofluorescent staining of α -SMA in hVSMCs, which treated with the above four different supernatant to investigate the hVSMCs morphology four find out the effect on hVSMC dedifferentiation. CXCR1/2 antagonist could inhibit the function of CXCL8. When treated with the CXCR1/2 antagonist, hVSMC morphology remain spindle in CM-HTR/8-SVneo^{shNC} and CM-HTR/8-SVneo^{shDAB2} group. The CM-HTR/8-SVneo^{shNC}+DMSO group hVSMC turn to round and consistent with the previous results. At the same time, the CM-HTR/8-SVneo^{shDAB2}+DMSO group hVSMC remain spindle shape. **b** The relative protein level (MYH-11, α -SMA) were detected by WB. The contractile indicators were not downregulated after co-cultured with CXCR1/2 antagonist. The CM-HTR/8-SVneo^{shNC}+DMSO group find that could promote hVSMC dedifferentiation (CM-HTR/8-SVneo^{shDAB2}+DMSO vs CM-HTR/8-SVneo^{shNC}+CXCR1/2 antagonist vs CM-HTR/8-SVneo^{shNC}+DMSO group vs CM-HTR/8-SVneo^{shDAB2}+CXCR1/2 antagonist: MYH-11: 1.011±0.245 vs 0.924±0.1422 vs 0.583±0.054 vs 1.294±0.029, $p^* < 0.05$; α -SMA: 1.162±0.223 vs 0.983±0.101 vs 0.611±0.014 vs 1.291±0.147, $p^* < 0.05$, $p^{**} < 0.01$). Moreover, AKT and pAKT two molecular in PI3K pathway were detected by WB analysis (CM-HTR/8-SVneo^{shDAB2}+DMSO vs CM-HTR/8-SVneo^{shNC}+CXCR1/2 antagonist vs CM-HTR/8-SVneo^{shNC}+DMSO group vs CM-HTR/8-SVneo^{shDAB2}+CXCR1/2 antagonist: p-AKT: 1.141±0.192 vs 0.639±0.068 vs 1.283±0.383 vs 0.767±0.064, $p^* < 0.05$; p-AKT/AKT: 0.959±0.1278 vs 0.616±0.094 vs 1.903±0.230 vs 0.7575±0.1468, $p^* < 0.05$). n=3. **c** Cell immunofluorescent staining of α -SMA in hVSMCs, which treated with the above four different supernatant to investigate the hVSMC morphology four find out the effect on hVSMCs dedifferentiation. When treated with the LY29400, hVSMCs morphology remain spindle in CM-HTR/8-SVneo^{shNC} and CM-HTR/8-SVneo^{shDAB2} group. The CM-HTR/8-SVneo^{shNC}+DMSO group hVSMC turn to round and consistent with the previous results. At the same time, the CM-HTR/8-SVneo^{shDAB2}+DMSO group hVSMCs remain spindle. **d** The relative protein level (MYH-11, α -SMA) were detected by WB. The contractile indicators were not downregulated after co-cultured with LY29400 (CM-HTR/8-SVneo^{shDAB2}+DMSO vs CM-HTR/8-SVneo^{shNC}+LY29400 vs CM-HTR/8-SVneo^{shNC}+DMSO group vs CM-HTR/8-SVneo^{shDAB2}+LY29400: MYH-11: 0.890±0.071 vs 0.870±0.066 vs 0.616±0.030 vs 1.11±0.032, $p^{**} < 0.01$; α -SMA: 0.890±0.061 vs 0.782±0.041 vs 0.525±0.049 vs 1.22±0.040, $p^{**} < 0.01$). pAKT was decreased when treated with LY29400 (CM-HTR/8-SVneo^{shDAB2}+DMSO vs CM-HTR/8-SVneo^{shNC}+LY29400 vs CM-HTR/8-SVneo^{shNC}+DMSO group vs CM-HTR/8-SVneo^{shDAB2}+LY29400: p-AKT: 0.875±0.094 vs 0.379±0.139 vs 1.592±0.344 vs 0.523±0.034, $p^* < 0.05$, $p^{**} < 0.01$; p-AKT/AKT: 1.079±0.1215 vs 0.399±0.127 vs 1.560±0.099 vs 0.508±0.2168, $p^* < 0.05$). n=3. **e** In order to further verify the critical role of CXCL8, exogenous factors of CXCL8 were added to different supernatants to observe whether CXCL8 could restore the dedifferentiated phenotype of the supernatant in the CM-HTR/8/SVneo^{shDAB2} group. The results showed that after CXCL8 was added to the supernatant in the knockout group, the cells turned round. The results suggest that CXCL8 is one of the key factors in dedifferentiation of hVSMC. **f** Consistent with the results of cell fluorescence, the differentiation index decreased after the addition of CXCL8 (CM-HTR/8-SVneo^{shDAB2}+DMSO vs CM-HTR/8-SVneo^{shNC}+CXCL8 vs CM-HTR/8-SVneo^{shNC}+DMSO group vs CM-HTR/8/SVneo^{shDAB2}+CXCL8: MYH-11: 1.044±0.032 vs 0.603±0.145 vs 0.457±0.155 vs 0.460±0.047, $p^{**} < 0.01$; α -SMA: 0.858±0.042 vs 0.629±0.042 vs 0.493±0.066 vs 0.508±0.012, $p^{**} < 0.01$, ns means there was no difference between them). n=3

limited size of our sequencing sample, which may affect the generalizability of our findings. In the control group, we selected samples from women who had preterm birth, which may introduce some bias. Additionally, the absence of spatiotemporal expression data for DAB2 limits our ability to precisely delineate its role throughout the different stages of EOPE. Understanding the temporal and spatial dynamics of DAB2 expression is crucial for fully comprehending its function in placental development and pathology. Moreover, our study predominantly relies on in vitro models. While these models are invaluable for dissecting molecular pathways and cellular interactions, they cannot replicate the complexity of in vivo systems. Therefore, there is a pressing need for comprehensive in vivo studies to confirm and extend our findings.

In conclusion, our study substantially enhances the understanding of placental biology and EOPE, particularly highlighting the complex mechanisms underlying spiral artery remodeling. The role of DAB2 in this process, as evidenced by its influence on EVT and hVSMC interactions, opens new avenues for maternal–fetal medicine research. Future studies should focus on elucidating the comprehensive role of DAB2 in various aspects of EOPE pathology, including its impact on immune responses and its potential as a biomarker for early detection and prognosis. Additionally, translating these findings into clinical practice remains a challenge. Potential therapeutic strategies, such as targeted inhibition of DAB2-mediated pathways or modulation of chemokine signaling, could pave the way for novel treatments for EOPE. These approaches might also provide insights into the management of other placental disorders and complications related to impaired vascular remodeling.

Supplementary Information The online version contains supplementary material available at <https://doi.org/10.1007/s00018-024-05212-4>.

Acknowledgements We sincerely thank the Springer Nature Author Services for editing the English text of a draft of this manuscript.

Author contributions D.J.C. and J.S.C. jointly conceived and supervised the project, interpreted the data, and revised the manuscript. Y.L. participated in writing the paper and prepared the figures. Y.L. and J.S.C. followed up with the patient, interpreted the clinical data, and participated in draft preparation. J.S.C. performed the scRNA-seq and data analysis. M.S.H., L.J.H., J.Y.L., S.F.G., and S.Y.L. managed the patient and collected clinical information. M.S.H., L.J.H., and J.Y.L. helped with sample collection and processing. S.Z., Z.W.T., and W.S. participated in the data analysis. All the authors have read and approved the final manuscript and declare no conflicts of interest.

Funding This work was supported by Grants from the National Natural Science Foundation of China (No. 81830045, 82071652, 81971414, and 81730040); the National Key R&D Program of China (No. 2022YFC2704500, 2022YFC2704505); the Project jointly funded by Guangzhou Science and Technology Plan, Guangzhou University (Institute) (202102010005); the National Science Foundation of

Guangdong Province (No. 2022A151505); and the Guangzhou School (college) Enterprise Joint Qualification Project (SL2022A03J00891).

Data availability The data supporting the findings of this study are found in the article and the supplementary material. The corresponding author will make all relevant raw data available upon reasonable request.

Declarations

Conflict of interest There are no competing financial or nonfinancial interests regarding this work.

Ethical approval The study received approval from the Medical Ethics Committee at The Third Affiliated Hospital of Guangzhou Medical University (Ethics Code: Medical Research No. 2020090). All participating women provided written informed consent.

Consent for publication All the authors have consented to publication.

Open Access This article is licensed under a Creative Commons Attribution 4.0 International License, which permits use, sharing, adaptation, distribution and reproduction in any medium or format, as long as you give appropriate credit to the original author(s) and the source, provide a link to the Creative Commons licence, and indicate if changes were made. The images or other third party material in this article are included in the article's Creative Commons licence, unless indicated otherwise in a credit line to the material. If material is not included in the article's Creative Commons licence and your intended use is not permitted by statutory regulation or exceeds the permitted use, you will need to obtain permission directly from the copyright holder. To view a copy of this licence, visit <http://creativecommons.org/licenses/by/4.0/>.

References

- Graham JB, Christopher WR, James MR, Ashley M (2019) Pre-eclampsia: pathophysiology and clinical implications. *BMJ* 366:12381
- Gardiner C, Vatish M (2017) Impact of haemostatic mechanisms on pathophysiology of preeclampsia. *Thromb Res* 151(Suppl 1):S48–S52
- Roberts JM, Rich-Edwards JW, McElrath TF, Garmire L, Myatt L (2021) Subtypes of preeclampsia: recognition and determining clinical usefulness. *Hypertension* 77(5):1430–1441
- Gupta AK, Gebhardt S, Hillermann R, Holzgreve W, Hahn S (2006) Analysis of plasma elastase levels in early and late onset preeclampsia. *Arch Gynecol Obstet* 273(4):239–242
- Gogoi P, Sinha P, Gupta B, Fimal P, Rajaram S (2019) Neutrophil-to-lymphocyte ratio and platelet indices in pre-eclampsia. *Int J Gynaecol Obstet* 144(1):16–20
- Oylumlu M, Ozler A, Yildiz A, Oylumlu M, Acet H, Polat N, Soyuncu HE, Yuksel M, Ertas F (2014) New inflammatory markers in pre-eclampsia: echocardiographic epicardial fat thickness and neutrophil to lymphocyte ratio. *Clin Exp Hypertens* 36(7):503–507
- Gezer C, Ekin A, Ertas IE, Ozeren M, Solmaz U, Mat E, Taner CE (2016) High first-trimester neutrophil-to-lymphocyte and platelet-to-lymphocyte ratios are indicators for early diagnosis of preeclampsia. *Ginekol Pol* 87(6):431–435
- Phillips C, Boyd M (2016) Assessment, management, and health implications of early-onset preeclampsia. *Nurs Womens Health* 20(4):400–414
- Huppertz B (2018) The critical role of abnormal trophoblast development in the etiology of preeclampsia. *Curr Pharm Biotechnol* 19(10):771–780
- Kam EPY, Gardner L, Loke YW, King A (1999) The role of trophoblast in the physiological change in decidual spiral arteries. *Hum Reprod* 14(8):2131–2138
- Robson A, Lash GE, Innes BA, Zhang JY, Robson SC, Bulmer JN (2019) Uterine spiral artery muscle dedifferentiation. *Hum Reprod* 34(8):1428–1438
- Harris LK (2011) IFPA Gabor Than Award lecture: transformation of the spiral arteries in human pregnancy: key events in the remodelling timeline. *Placenta* 32(Suppl 2):S154–S158
- Whitley GS, Cartwright JE (2010) Cellular and molecular regulation of spiral artery remodelling: lessons from the cardiovascular field. *Placenta* 31(6):465–474
- Hering L, Herse F, Verlohren S, Park J-K, Wellner M, Qadri F, Pijnenborg R, Staff AC, Huppertz B, Muller DN et al (2008) Trophoblasts reduce the vascular smooth muscle cell proatherogenic response. *Hypertension* 51(2):554–559
- Aldo PB, Krikun G, Visintin I, Lockwood C, Romero R, Mor G (2007) A novel three-dimensional in vitro system to study trophoblast-endothelium cell interactions. *Am J Reprod Immunol* 58(2):98–110
- Lindschau C, Quass P, Menne J, Güler F, Fiebeler A, Leitges M, Luft FC, Haller H (2003) Glucose-induced TGF-beta1 and TGF-beta receptor-1 expression in vascular smooth muscle cells is mediated by protein kinase C-alpha. *Hypertension* 42(3):335–341
- Lu QB, Wan MY, Wang PY, Zhang CX, Xu DY, Liao X, Sun HJ (2018) Chicoric acid prevents PDGF-BB-induced VSMC dedifferentiation, proliferation and migration by suppressing ROS/NFkB/mTOR/P70S6K signaling cascade. *Redox Biol* 14:656–668
- Owens GK (2007) Molecular control of vascular smooth muscle cell differentiation and phenotypic plasticity. *Novartis Found Symp* 283:174–191
- Pijnenborg R, Vercruyse L, Hanssens M (2006) The uterine spiral arteries in human pregnancy: facts and controversies. *Placenta* 27(9–10):939–958
- Zhou J, Hsieh JT (2001) The inhibitory role of DOC-2/DAB2 in growth factor receptor-mediated signal cascade. DOC-2/DAB2-mediated inhibition of ERK phosphorylation via binding to Grb2. *J Biol Chem* 276(30):27793–27798
- Morris SM, Arden SD, Roberts RC, Kendrick-Jones J, Cooper JA, Luzio JP, Buss F (2002) Myosin VI binds to and localises with Dab2, potentially linking receptor-mediated endocytosis and the actin cytoskeleton. *Traffic* 3(5):331–341
- Rosenbauer F, Kallies A, Scheller M, Knobloch KP, Rock CO, Schwieger M, Stocking C, Horak I (2002) Disabled-2 is transcriptionally regulated by ICSBP and augments macrophage spreading and adhesion. *Embo j* 21(3):211–220
- Mok SC, Wong KK, Chan RK, Lau CC, Tsao SW, Knapp RK, Berkowitz RS (1994) Molecular cloning of differentially expressed genes in human epithelial ovarian cancer. *Gynecol Oncol* 52(2):247–252
- Huang Y, Friess H, Kleeff J, Esposito I, Zhu Z, Liu S, Mok SC, Zimmermann A, Büchler MW (2001) Doc-2/hDab2 expression is up-regulated in primary pancreatic cancer but reduced in metastasis. *Lab Invest* 81(6):863–873
- Kleeff J, Huang Y, Mok SC, Zimmermann A, Friess H, Büchler MW (2002) Down-regulation of DOC-2 in colorectal cancer points to its role as a tumor suppressor in this malignancy. *Dis Colon Rectum* 45(9):1242–1248
- Anupam K, Tusharkant C, Gupta SD, Ranju R (2006) Loss of disabled-2 expression is an early event in esophageal squamous tumorigenesis. *World J Gastroenterol* 12(37):6041–6045

27. Zhang S, Ding J, Zhang Y, Liu S, Yang J, Yin T (2022) Regulation and function of chemokines at the maternal–fetal interface. *Front Cell Dev Biol* 10:826053
28. Sato Y, Higuchi T, Yoshioka S, Tatsumi K, Fujiwara H, Fujii S (2003) Trophoblasts acquire a chemokine receptor, CCR1, as they differentiate towards invasive phenotype. *Development* 130(22):5519–5532
29. Zhang L, Liu J, Feng X, Lash GE (2023) Unraveling the mysteries of spiral artery remodeling. *Placenta* 141:51–56
30. Kaimoto T, Yasuda O, Ohishi M, Mogi M, Takemura Y, Suhara T, Ogihara T, Fukuo K, Rakugi H (2010) Nifedipine inhibits vascular smooth muscle cell dedifferentiation via downregulation of Akt signaling. *Hypertension* 56(2):247–252
31. Lee CK, Lee HM, Kim HJ, Park HJ, Won KJ, Roh HY, Choi WS, Jeon BH, Park TK, Kim B (2007) Syk contributes to PDGF-BB-mediated migration of rat aortic smooth muscle cells via MAPK pathways. *Cardiovasc Res* 74(1):159–168
32. Surazynski A, Donald SP, Cooper SK, Whiteside MA, Salnikow K, Liu Y, Phang JM (2008) Extracellular matrix and HIF-1 signaling: the role of prolydase. *Int J Cancer* 122(6):1435–1440
33. Owens GK, Kumar MS, Wamhoff BR (2004) Molecular regulation of vascular smooth muscle cell differentiation in development and disease. *Physiol Rev* 84(3):767–801
34. Liu H, Ning F, Lash GE (2022) Contribution of vascular smooth muscle cell apoptosis to spiral artery remodeling in early human pregnancy. *Placenta* 120:10–17
35. Wu D, Liu Y, Liu X, Liu W, Shi H, Zhang Y, Zou L, Zhao Y (2020) Heme oxygenase-1 gene modified human placental mesenchymal stem cells promote placental angiogenesis and spiral artery remodeling by improving the balance of angiogenic factors in vitro. *Placenta* 99:70–77
36. Brazil DP, Yang Z-Z, Hemmings BA (2004) Advances in protein kinase B signalling: AKTion on multiple fronts. *Trends Biochem Sci* 29(5):233–242
37. Wang H, Zhong B, Geng Y, Hao J, Jin Q, Zhang Y, Dong L, Gao D, Li J, Hou W (2021) TIPE2 inhibits PDGF-BB-induced phenotype switching in airway smooth muscle cells through the PI3K/Akt signaling pathway. *Respir Res* 22(1):238
38. Han ZJ, Li YB, Yang LX, Cheng HJ, Liu X, Chen H (2021) Roles of the CXCL8-CXCR1/2 Axis in the tumor microenvironment and immunotherapy. *Molecules* 27(1):137
39. Crosas-Molist E, Samain R, Kohlhammer L, Orgaz JL, George SL, Maiques O, Barcelo J, Sanz-Moreno V (2021) Rho GTPase signaling in cancer progression and dissemination. *Physiol Rev* 102(1):455–510
40. Socha MW, Malinowski B, Puk O, Wartęga M, Stankiewicz M, Kazdepka-Ziemińska A, Wiciński M (2021) The role of NF-κB in uterine spiral arteries remodeling, insight into the cornerstone of preeclampsia. *Int J Mol Sci* 22(2):704
41. Côté AM, Firoz T, Mattman A, Lam EM, von Dadelszen P, Magee LA (2008) The 24-hour urine collection: gold standard or historical practice? *Am J Obstet Gynecol* 199(6):625.e621–626
42. Menzies J, Magee LA, Macnab YC, Ansermino JM, Li J, Douglas MJ, Gruslin A, Kyle P, Lee SK, Moore MP et al (2007) Current CHS and NHBPEP criteria for severe preeclampsia do not uniformly predict adverse maternal or perinatal outcomes. *Hypertens Pregnancy* 26(4):447–462
43. Ogbu SC, Musich PR, Zhang J, Yao ZQ, Howe PH, Jiang Y (2021) The role of disabled-2 (Dab2) in diseases. *Gene* 769:145202
44. Price ZK, Lokman NA, Yoshihara M, Kajiyama H, Oehler MK, Ricciardelli C (2022) Disabled-2 (DAB2): a key regulator of anti- and pro-tumorigenic pathways. *Int J Mol Sci* 24(1):696
45. Wang H, Dong S, Liu Y, Ma F, Fang J, Zhang W, Shao S, Shen H, Jin J (2020) DAB2 suppresses gastric cancer migration by regulating the Wnt/β-catenin and hippo-YAP signaling pathways. *Transl Cancer Res* 9(2):1174–1184
46. Teckchandani A, Toida N, Goodchild J, Henderson C, Watts J, Wollscheid B, Cooper JA (2009) Quantitative proteomics identifies a Dab2/integrin module regulating cell migration. *J Cell Biol* 186(1):99–111
47. Drake PM, Fisher SJ, Red-Horse K (2004) Human pregnancy: the role of chemokine networks at the fetal–maternal interface. *Expert Rev Mol Med* 6(11):1–14
48. Du MR, Wang SC, Li DJ (2014) The integrative roles of chemokines at the maternal–fetal interface in early pregnancy. *Cell Mol Immunol* 11(5):438–448
49. Choudhury RH, Dunk CE, Lye SJ, Aplin JD, Harris LK, Jones RL (2017) Extravillous trophoblast and endothelial cell crosstalk mediates leukocyte infiltration to the early remodeling decidual spiral arteriole wall. *J Immunol* 198(10):4115–4128
50. Cavanagh PC, Dunk C, Pampillo M, Szereszewski JM, Taylor JE, Kahiri C, Han V, Lye S, Bhattacharya M, Babwah AV (2009) Gonadotropin-releasing hormone-regulated chemokine expression in human placentation. *Am J Physiol Cell Physiol* 297(1):C17–27
51. Jovanović M, Stefanoska I, Radojčić L, Vićovac L (2010) Interleukin-8 (CXCL8) stimulates trophoblast cell migration and invasion by increasing levels of matrix metalloproteinase (MMP)2 and MMP9 and integrins alpha5 and beta1. *Reproduction* 139(4):789–798
52. Liu HB, Bai J, Wang WX (2023) CST1 promotes the proliferation and migration of PDGF-BB-treated airway smooth muscle cells via the PI3K/AKT signaling pathway. *Kaohsiung J Med Sci* 39(2):145–153
53. Chen S, Dong S, Li Z, Guo X, Zhang N, Yu B, Sun Y (2017) Atorvastatin calcium inhibits PDGF-β-induced proliferation and migration of VSMCs through the G0/G1 cell cycle arrest and suppression of activated PDGFRβ-PI3K-Akt signaling cascade. *Cell Physiol Biochem* 44(1):215–228
54. Ren Y, Li R, Zheng Y, Busch H (1998) Cloning and characterization of GEF-H1, a microtubule-associated guanine nucleotide exchange factor for Rac and Rho GTPases. *J Biol Chem* 273(52):34954–34960
55. Huang Z, Du G, Huang X, Han L, Han X, Xu B, Zhang Y, Yu M, Qin Y, Xia Y et al (2018) The enhancer RNA Inc-SLC4A1-1 epigenetically regulates unexplained recurrent pregnancy loss (URPL) by activating CXCL8 and NF-κB pathway. *EBioMedicine* 38:162–170
56. Guo F, Tang J, Zhou Z, Dou Y, Van Lonkhuyzen D, Gao C, Huan J (2012) GEF-H1-RhoA signaling pathway mediates LPS-induced NF-κB transactivation and IL-8 synthesis in endothelial cells. *Mol Immunol* 50(1–2):98–107

Publisher's Note Springer Nature remains neutral with regard to jurisdictional claims in published maps and institutional affiliations.